Table V. Local-Mode Parameters for O–H Oscillators in $BaCl_2 \cdot 2X_2O$ (X = H, D)[a]

	H_2O[b]		HOD	
oscillator	X	ω	X	ω
1	−169	3656	−135	3626
2	−149	3659	−141	3587
3	−151	3629	−138	3596
4	−96	3650	−103	3667

[a] Data in cm^{-1}. [b] Calculated only from $v = 1$ and $v = 2$ data.

sample. This behavior is expected, since the probability of having two O–H in the same molecule will be extremely small in the 98% deuterated crystal.

It should be noted that the assignments of the bands at 6688 and 6712 cm^{-1} are the opposite of those reported previously.[2] The best fit based on a more extensive data set using the Newton–Raphson minimization gives a reverse assignment of these bands. This nicely illustrates the help that deuteration studies can give to the unambiguous assignment of bands in a complicated vibrational spectrum.

The shift of the bands to higher energy on deuteration indicates that replacement of one O–H oscillator in H_2O by O–D has a significant effect on the local-mode parameters of the remaining O–H oscillator. The extent to which these shifts on deuteration alter the local-mode parameters can be seen from the data in Table V, in which we list local-mode parameters calculated from the four OH stretches and four OH overtone bands of HOD. These are compared with the corresponding parameters calculated for $BaCl_2 \cdot 2H_2O$ by using only the 10 bands observed for the $v = 1$ and $v = 2$ data set. In going from H_2O to HOD, there is generally a decrease in ω and in the numerical magnitude of X. Oscillator 4, the bifurcated hydrogen bond, is the exception.

While the following is highly speculative, it may offer some partial explanation of these observations. Robertson's[18] extensive calculations on the system $(CH_3)_2O \cdots HCl$ (or DCl) predict that the O···Cl distance should be 1.8 pm longer in the DCl system. Likewise, in many hydrogen-bonded crystals the A–B distance in A–D···B is found to be slightly longer (ca. 1–4 pm) than that in A–H···B.[19] Although the distances in $BaCl_2 \cdot 2D_2O$ have not been reported, if we assume that there is an increase in the O···Cl distance on deuteration, then in a highly deuterated crystal the residual O–H oscillators would experience the longer O···Cl distance, and this would be reflected in a slight weakening of the O–H···Cl hydrogen bond and a smaller value of X. Other explanations, however, are also possible. For example, Fermi resonance between the $\nu + 2\delta$ and 2ν features of H_2O could cause the $|20\rangle$ and $|02\rangle$ bands of H_2O to be lower in energy than the corresponding bands in HOD. In the latter there would be little Fermi resonance, since the δ(HOD) vibrations are at 1410, 1427, and 1460 cm^{-1}, while the $\delta(H_2O)$ vibrations are at 1600 and 1641 cm^{-1}.[7]

Conclusions. The simplicity of the model used in this study does not permit very refined conclusions to be drawn from the data. The following statements, however, appear to be warranted. (1) The ratio ω_D/ω_H for water in BCD correlates almost exactly with that calculated from the masses of the atoms in the OD and OH bonds. Because of hydrogen bonding the values of ω_D and ω_H in BCD are both lower than in gaseous D_2O and H_2O. (2) In deuterated as well as nondeuterated BCD one X value is significantly smaller than the other three. This corresponds to the weakly hydrogen-bonded oscillator 4. (3) The λ values for coordinated D_2O (H_2O) are smaller than those for gaseous D_2O (H_2O). This is due mainly to smaller values of the potential coupling term, which is linked to constrained movement of the hydrogen-bonded H (or D) atom. (4) The value of λ for coordinated D_2O is larger than that for coordinated H_2O. This follows the trend in gas-phase water and is a consequence of the Wilson g_{ij} term. (5) The 2ν(OH) bands of HOD in deuterated crystals of BCD lie at higher energy than 2ν(OH) of H_2O. Accordingly, the local-mode parameters of HOD are perceptibly different from those of H_2O in this crystal.

Acknowledgment. I.M.W. thanks the National Science and Engineering Research Council of Canada for financial assistance. P.J.M. thanks the Research Corp. for a grant to purchase the cryogenic refrigerator.

---

[18] Robertson, G. N. *Philos. Trans. R. Soc. (London)* **1977**, *A286*, 25.

[19] Ubbelohde, A. R.; Gallagher, K. J. *Acta Crystallogr.* **1955**, *8*, 71.

Contribution from the Department of Chemistry,
Emory University, Atlanta, Georgia 30322

Comparative Study of Polyoxometalates and Semiconductor Metal Oxides as Catalysts. Photochemical Oxidative Degradation of Thioethers

R. Carlisle Chambers and Craig L. Hill*

Received May 23, 1990

The photochemical degradation of thioether substrates catalyzed by representative semiconductor metal oxides and sulfides (anatase TiO_2, SnO_2, cubic WO_3, and CdS) and photoredox-active early-transition-metal polyoxometalates ($W_{10}O_{32}^{4-}$, $PMo_{12}O_{40}^{3-}$, $PW_{12}O_{40}^{3-}$, $SiMo_{12}O_{40}^{4-}$, $PV_2Mo_{10}O_{40}^{5-}$, $Cu^{II}W_{11}PO_{39}^{5-}$, and $P_2W_{18}O_{62}^{6-}$) have been examined under both anaerobic and aerobic conditions. Under anaerobic conditions, all the semiconductors are completely ineffective at photochemically oxidizing or degrading the exemplary thioether substrate tetrahydrothiophene (THT) in the oxidatively resistant solvent acetonitrile. In contrast, all the homogeneous polyoxometalate systems under the same reaction conditions, except the neutral tetra-*n*-butylammonium (Q) salt of $PW_{12}O_{40}^{3-}$, are quite effective. The latter systems generate products derived from the carbon-based radical α to the sulfur atom and not sulfoxide or sulfone, the usual products of thioether oxidation by oxometal species. The rate for the most active anaerobic system, that involving the photochemical degradation of THT by $Q_4W_{10}O_{32}$, under optically dilute conditions, is first order in $W_{10}O_{32}^{4-}$ and light intensity and variable order in THT substrate. A rate law consistent with these data is given. Upon addition of O_2, TiO_2 (with or without Pt(0)) becomes highly active, SnO_2 becomes active, but WO_3 and CdS remain inactive. Reactivity in thioether oxidation is dominated by the interactions of the semiconductors with O_2 and O_2-derived intermediates; there is no correlation between reactivity and semiconductor band gap. Upon addition of O_2, all the polyoxometalate systems become more active. Both the semiconductors and polyoxometalates under aerobic conditions oxidize thioethers further than the sulfoxides or sulfones to a range of products.

Introduction

Several of the structural, electronic, and photochemical features of many semiconductor metal oxides parallel those of some families of early-transition-metal polyoxometalates. Both classes of materials exhibit a rich photoinduced redox chemistry and can catalyze the photochemical modification of a range of organic

0020-1669/91/1330-2776$02.50/0

materials.[1-7] The generally accepted pathways in the photochemical dehydrogenation (anaerobic conditions) or photooxidation (aerobic conditions) of organic substrates by polyoxometalates are illustrated in eqs 1–6,[3-6] where $\mathrm{P_{ox}}$ = ground state of the

$$\mathrm{P_{ox}} + h\nu \longrightarrow \mathrm{P_{ox}}^* \tag{1}$$

$$\mathrm{P_{ox}}^* + \mathrm{P_{ox}} + \mathrm{SH_2} \longrightarrow 2\,\mathrm{P_{red}} + \mathrm{S} + 2\mathrm{H^+} \tag{2}$$

$$2\,\mathrm{P_{red}} + 2\mathrm{H^+} \longrightarrow 2\,\mathrm{P_{ox}} + \mathrm{H_2} \tag{3}$$

net reaction from eq 1-3:

$$\mathrm{SH_2} + h\nu \xrightarrow[\text{(catalyst)}]{\mathrm{P_{ox}}} \mathrm{S} + \mathrm{H_2} \tag{4}$$

$$2\,\mathrm{P_{red}} + 2\,\mathrm{H^+} + 1/2\,\mathrm{O_2} \longrightarrow 2\,\mathrm{P_{ox}} + \mathrm{H_2O} \tag{5}$$

net reaction from eq 1,2 & 5:

$$\mathrm{SH_2} + 1/2\,\mathrm{O_2} + h\nu \xrightarrow[\text{(catalyst)}]{\mathrm{P_{ox}}} \mathrm{S} + \mathrm{H_2O} \tag{6}$$

oxidized form of polyoxometalate catalyst (e.g. α-$\mathrm{PW_{12}O_{40}}^{3-}$, α-$\mathrm{P_2W_{18}O_{62}}^{6-}$, $\mathrm{W_{10}O_{32}}^{4-}$, etc.), $\mathrm{P_{red}}$ = ground state of the reduced form of polyoxometalate catalyst (e.g. α-$\mathrm{PW_{12}O_{40}}^{4-}$, α-$\mathrm{P_2W_{18}O_{62}}^{7-}$, $\mathrm{W_{10}O_{32}}^{5-}$, etc.), $\mathrm{SH_2}$ = organic substrate = alcohols, amides, ethers, hydrocarbons, and others, and S = oxidized organic product. Clearly the absorption of light by the ground electronic state of the d^0 polyoxometalate ($\mathrm{P_{ox}}$) producing the charge-transfer-excited state ($\mathrm{P_{ox}}^*$) is qualitatively analogous to the absorption of band gap radiation by a d^0 semiconductor metal oxide producing a transient electron–hole pair. Likewise substrate oxidation by the excited state of the polyoxometalate, eq 2, is analogous to the corresponding process in semiconductors. Catalytic cycles in which the initial forms of the polyoxometalate or semiconductor catalyst are regenerated by catalyzed hydrogen evolution or reoxidation by $\mathrm{O_2}$ or $\mathrm{O_2}$-derived species are somewhat analogous.[1-6] Examination of the literature on semiconductor-based photochemical oxidation of organic compounds and numerous experiments in our laboratory,[8] however, indicate that, with most metal oxide semiconductors, there is virtually no net oxidative transformation of organic substrates in the absence of $\mathrm{O_2}$. This is in marked contrast to the polyoxometalate systems.[3-6]

In this study we examine the photochemical degradation of organic substrates by representative semiconductor metal oxides and polyoxometalates under both anaerobic and aerobic conditions for the first time.[3] The catalytic photochemical degradation of toxic organic materials, including halocarbons, by both semiconductors[2] and polyoxometalates,[7] although a relatively new and growing area, is already of commercial importance. Thioethers (organic sulfides) were chosen as the substrates in this study, as they are readily oxidized, their well-defined oxidation products are indicative of mechanism, and several thioethers are toxic and are the focus of current research on catalytic methods of decontamination.[9] The anaerobic reaction conditions used in this study were essential in the evaluation of mechanism, as the myriad of oxidation processes possible in the presence of $\mathrm{O_2}$, including the dominant radical-chain mechanisms, can obscure the inherent reactions between the excited state of the polyoxometalate or semiconductor and the substrate.

Experimental Section

Materials. The solvents were obtained, purified, and manipulated as described earlier.[4,5] The thioether substrates tetrahydrothiophene (THT) and dimethyl sulfide along with their sulfoxides and sulfones were Aldrich reagent grade and were used without further purification. The dithiane 2,5-dithiahexane was purchased from Columbia. Pivalonitrile (Lancaster) and bromobenzene (Aldrich) were used as internal standards. The polyoxometalate complexes α-$\mathrm{Q_3PW_{12}O_{40}}$,[10] $\mathrm{Q_3PMo_{12}O_{40}}$,[10] $\mathrm{Q_4W_{10}O_{32}}$,[11] $\mathrm{Q_4SiMo_{12}O_{40}}$,[10] $\mathrm{Q_5PV_2Mo_{10}O_{40}}$,[12] $\mathrm{H_5PV_2Mo_{10}O_{40}}$,[12] $\mathrm{Q_5Cu^{II}W_{11}PO_{39}}$,[13] and α-$\mathrm{(NH_4)_6P_2W_{18}O_{62}}$[14] (where Q = ($n$-$\mathrm{C_4H_9)_4N^+}$)) were prepared and purified by using literature procedures. $\mathrm{TiO_2}$ (anatase) was obtained from two different vendors: Degussa (P 25 grade) and Aldrich. $\mathrm{SnO_2}$ (Aldrich), CdS (Fluka), and $\mathrm{H_4PtCl_6}$ (Aldrich) were commercial samples and were used as received. Cubic $\mathrm{WO_3}$ was prepared by the procedure of Siedle and co-workers.[15] Platinization of the $\mathrm{TiO_2}$ was carried out by using $\mathrm{H_4PtCl_6}$ and the method of Bard.[16] Zero-Grade oxygen (ppm impurities of $\mathrm{H_2O}$, $\mathrm{CO_2}$, and hydrocarbons) and argon were both obtained from Linde.

Methods. In a typical reaction, 5.0 mL of an acetonitrile solution 10 mM in thioether and 9 mM in internal standard (pivalonitrile), along with the appropriate polyoxometalate or semiconductor (see Tables), were placed in a 30-mL Pyrex Schlenk flask fitted with a Teflon stopper.

---

(1) Recent reviews of semiconductor metal oxide mediated photochemical oxidations or transformations of organic substrates (see also references cited therein): (a) Fox, M. A. *Acc. Chem. Res.* **1983**, *16*, 314. (b) *Homogeneous and Heterogeneous Photocatalysis*: Pelizzetti, E., Serpone, N., Eds.; NATO ASI Series C, Vol. 174; Reidel: Dordrecht, The Netherlands, 1986. (c) Pichat, P.; Fox, M. A. In *Photoinduced Electron Transfer*; Elsevier: Amsterdam, 1988; Vol. D., pp 241–303. (d) Grätzel, M. *Heterogeneous Photochemical Electron Transfer*; CRC Press: Boca Raton, FL, 1989; Chapter 3. (e) *Photochemical Energy Conversion*; Norris, J. R., Jr.; Meisel, D. Eds.; Elsevier: New York, 1989; Part IV.

(2) Photochemical degradation of halocarbons and other toxic organic compounds catalyzed by semiconductor metal oxides: (a) Barbeni, N.; Pramauro, E.; Pelizzetti, E.; Borgarello, E.; Grätzel, M.; Serpone, N. *Nouv. J. Chim.* **1984**, *8*, 547. (b) Grätzel, C. K.; Jirousek, M.; Grätzel, M. *J. Mol. Catal.* **1987**, *39*, 347. (c) Hidaka, H.; Kubota, H.; Grätzel, M.; Serpone, N.; Pelizzetti, E. *Nouv. J. Chim.* **1985**, *9*, 67. (d) Serpone, N. In ref 1e, pp 297–315.

(3) Comparison of monomeric tungstate esters, polyoxotungstates, and tungstic oxide in the aerobic photooxidation of alcohols: Fox, M. A.; Cardona, R.; Gaillard, E. *J. Am. Chem. Soc.* **1987**, *109*, 6347.

(4) Polyoxometalate-catalyzed photochemical transformation of saturated hydrocarbons: (a) Renneke, R. F.; Hill, C. L. *J. Am. Chem. Soc.* **1986**, *108*, 3528; **1988**, *110*, 5461. (b) Shul'pin, G. B.; Kats, M. M.; Lederer, P.; Mácová, E. Abstracts of the 2nd All-Union Symposium on Homogeneous Catalysis, Donetsk, May 1988; p 75. Shul'pin, G. B.; Kats, M. M. *Zh. Obshch. Khim.* **1989**, *59*, 2738. (c) Chambers, R. C.; Hill, C. L. *Inorg. Chem.* **1989**, *28*, 2509. (d) Hill, C. L.; Renneke, R. F.; Combs, L. A. *New J. Chem.* **1989**, *13*, 701. (e) Prosser-McCartha, C. M.; Hill, C. L. *J. Am. Chem. Soc.* **1990**, *112*, 3671. (f) Renneke, R. F.; Pasquali, M.; Hill, C. L. *J. Am. Chem. Soc.* **1990**, *112*, 6585.

(5) Photosensitive or photocatalytic polyoxometalate–organic systems with electron donor–acceptor character: (a) Prosser–McCartha, C. M.; Kadkhodayan, M.; Williamson, M. M.; Bouchard, D. A.; Hill, C. L. *J. Chem. Soc., Chem. Commun.* **1986**, 1747. (b) Williamson, M. M.; Bouchard, D. A.; Hill, C. L. *Inorg. Chem.* **1987**, *26*, 1436. (c) Hill, C. L.; Bouchard, D. A.; Kadkhodayan, M.; Williamson, M. M.; Schmidt, J. A.; Hilinski, E. F. *J. Am. Chem. Soc.* **1988**, *110*, 5471.

(6) Recent representative papers on photooxidation of organic substrates other than alkanes by polyoxometalates listed alphabetically by principal investigator's last name: (a) Attanasio, D.; Suber, L.; Thorslund, K. *Inorg. Chem.* **1991**, *30*, 590. (b) Akid, R.; Darwent, J. R. *J. Chem. Soc., Dalton Trans.* **1985**, 395. (c) Kraut, B.; Ferraudi, G. *Inorg. Chem.* **1990**, *29*, 4843. (d) Hill, C. L.; Bouchard, D. A. *J. Am. Chem. Soc.* **1985**, *107*, 5148. (e) Nomiya, K.; Miyazaki, T.; Maeda, K.; Miwa, M. *Inorg. Chim. Acta* **1987**, *127*, 65. (f) Papaconstantinou, E. *Chem. Soc. Rev.* **1989**, *18*, 1. (g) Savinov, E. N.; Saidkhanov, S. S.; Parmon, V. N.; Zamaraev, K. I. *Dokl. Phys. Chem.* (*Engl. Transl.*) **1983**, *272*, 741. (h) Ward, M. D.; Brazdil, J. F.; Mehandu, S. P.; Anderson, A. B. *J. Phys. Chem.* **1987**, *91*, 6515. (i) Yamase, T.; Usami, T. *J. Chem. Soc., Dalton Trans.* **1988**, 183.

(7) Photochemical degradation of halocarbons by organic reductants catalyzed by polyoxometalates: (a) Sattari, D.; Hill, C. L. *J. Chem. Soc., Chem. Commun.* **1990**, 634. (b) Sattari, D.; Hill, C. L. Unpublished work. These complex reactions entail major processes other than eqs 1–6 in the text.

(8) For example, repeated attempts to photooxidize hydrocarbons by both untreated and Pt(0)-doped Degussa P 25 $\mathrm{TiO_2}$ and other semiconductors under anaerobic conditions have failed to produce any evidence of reaction.

(9) (a) Yang, Y.-C.; Szafraniec, L. L.; Beaudry, W. T.; Ward, J. R. *J. Org. Chem.* **1988**, *53*, 3293. (b) *Proceedings of the 1988 U.S. Army CRDEC Conference on Chemical Defense Research*; GPO: Washington, DC, 1989; Vol. I, Sections I and XVIII and references cited therein. (c) Yang, Y.-C.; Szafraniec, L. L.; Beaudry, W. T.; Rohrbaugh, D. K. *J. Am. Chem. Soc.* **1990**, *112*, 6621. (d) Menger, F. M.; Elrington, A. R. *J. Am. Chem. Soc.* **1990**, *112*, 8201.

(10) (a) Wu, H. *J. Biol. Chem.* **1920**, *43*, 189. (b) Filowitz, M.; Ho, R. K. C.; Klemperer, W. G.; Shum, W. *Inorg. Chem.* **1979**, *18*, 93.

(11) (a) Chemseddine, A.; Sanchez, C.; Livage, J.; Launay, J. P.; Fournier, M. *Inorg. Chem.* **1984**, *23*, 2609. (b) Renneke, R. F. Ph.D. Thesis, Emory University, 1989.

(12) Tsigdinos, G. A.; Hallada, C. J. *Inorg. Chem.* **1968**, *7*, 437.

(13) Tourné, C. M.; Tourné, G. F.; Malik, S. A.; Weakley, T. J. R. *J. Inorg. Nucl. Chem.* **1970**, *32*, 3875.

(14) Acerete, R. Ph.D. Thesis, Georgetown University, 1981.

(15) Siedle, A. R.; Wood, T. E.; Brostrom, M. L.; Koskermak, D. C.; Montez, B.; Oldfield, E. *J. Am. Chem. Soc.* **1989**, *111*, 1665.

(16) Kraeutler, B.; Bard, A. J. *J. Am. Chem. Soc.* **1978**, *100*, 4317.

After thorough degassing, the irradiation was begun by using either a Hanovia 550-W medium-pressure Hg lamp (for reactions >10 h) or an Oriel 1000-W ozone-free high-pressure Xe arc lamp equipped with infrared and λ >340 nm cutoff filters (for aerobic reactions). During irradiation, the reactions were vigorously stirred with a Teflon-covered stir bar and maintained at a constant temperature of 25 °C. Anaerobic reactions were maintained under ~1 atm of Ar. Aerobic reactions were conducted by adding 20 cm^3 of O_2 (Zero-Grade) (800 equiv relative to polyoxometalate) to the flask prior to irradiation.

Product analyses were conducted by using a Hewlett-Packard 5890 gas chromatograph equipped with a flame ionization detector and a 25 m × 0.2 mm 5% phenyl methyl silicone capillary column. Nitrogen was used as the carrier gas, and products were quantified by using a Hewlett-Packard 3390A integrator. The heterogeneous reaction mixtures were centrifuged prior to product analysis. Aliquots for analysis were drawn from the resulting solution. GC–mass spectroscopy analysis was performed by EcoTek Laboratories (Atlanta, GA).

Quantum Yield Measurements of Polyoxometalate Reduction and Dimethyl Sulfide Derived Oxidation Products. Experiments were conducted to measure the quantum yield at 320 nm for both reduction of the polyoxometalate catalyst and formation of organic products. Dimethyl sulfide was used as substrate, since its photolysis with $Q_4W_{10}O_{32}$ in CH_3CN gives only one product, 2,5-dithiahexane. The 1000-W Xe arc lamp setup described previously was used with an Oriel interference filter to isolate a band centered at 324 nm (T_{max} = 0.28%). The incident-light intensity (2.5 × 10^{-8} einstein/s) was measured by the method of Hatchard and Parker.[17] The quantum yields were determined by the prescribed ferrioxalate procedure with one exception.[11b,17] The procedure was modified by the addition of NH_4F in the workup of the photolyte from the ferrioxalate measurements.[18]

The polyoxometalate quantum yield measurements were carried out at 25 °C under inert atmosphere in a 1.0-cm quartz cuvette. Reaction mixtures contained a 5 mM concentration of the particular polyoxometalate and 0.5 M dimethyl sulfide in 2 mL of CH_3CN. Formation of the reduced polyoxoanion species was monitored by UV spectroscopy. A microprocessor-controlled Hewlett-Packard 8451A multidiode array UV–visible instrument was used in these experiments. For organic product formation, 9 mM internal standard (bromobenzene) was added to 1 mL of the photolyte, followed by GC analysis. A value of Φ = 1.24 at 320 nm was used for the ferrioxalate actinometer to determine the quantum yields directly.[17a]

Kinetic Measurements of Reduced Decatungstate and Tetrahydrothiophene. Kinetic experiments involving $Q_4W_{10}O_{32}$ and THT in CH_3CN were carried out at 25 °C by using a 2.0 mm path length quartz cylindrical Schlenk cuvette irradiated with the 1000-W Xe arc lamp source. The kinetic measurements involved monitoring the initial rate of formation of the two-electron-reduced species, $W_{10}O_{32}^{6-}$ (λ_{max} = 630 nm, ϵ = 12 500 cm^{-1} M^{-1} in CH_3CN),[11b] in the absorption spectrum. Reproducible rate behavior was obtained at low conversions of substrate. The rate of reoxidation of the reduced form of the complex was at least 2 orders of magnitude slower than the forward reaction, photooxidation of THT substrate with reduction of the polyoxotungstate. The rate dependence on light intensity was determined by using neutral-density filters placed between the light source with an IR filter and the sample. In several thioether photooxidation reactions, substantial quantities of the reduced decatungstate species were generated by photooxidation of the CH_3CN solvent. All rate data were corrected for this background solvent photooxidation process.

Results and Discussion

The relative abilities of a range of polyoxometalates and semiconductor metal oxides to photooxidize thioethers under both anaerobic and aerobic conditions have been examined. Representative polyoxometalates in three structural classes, decatungstate (D_{4h} symmetry), Keggin (T_d symmetry), and Wells–Dawson (α isomer, D_{3h} symmetry), with varying ground-state redox potentials have been synthesized and purified, principally as their tetra-*n*-butylammonium salts, and used in these experiments. The following metal oxide and sulfide semiconductors in powder form were obtained and used: (1) TiO_2 (anatase) from Aldrich, (2) TiO_2 (anatase) from Degussa (P 25), generally believed to be the most effective semiconductor metal oxide for organic photooxidations,[2,19] (3) cubic WO_3, the semiconductor corresponding to the most effective polyoxometalates in these photooxidation reactions, the decatungstates,[20] (4) SnO_2, and (5) CdS, a semiconducting metal sulfide.

Table I. Photochemical Decomposition of Tetrahydrothiophene (THT) under Anaerobic Conditions Catalyzed by Various Catalysts[a]

catalyst	mole ratio[b]	% decompn[c]
Polyoxometalate Systems		
$Q_4W_{10}O_{32}$	20	41
$Q_3PMo_{12}O_{40}$	10	11
$Q_3PW_{12}O_{40}$	10	0
$Q_4SiMo_{12}O_{40}$	10	14
$Q_5PV_2Mo_{10}O_{40}$	10	12
$H_5PV_2Mo_{10}O_{40}$	10	12
$Q_5Cu^{II}W_{11}PO_{39}$	10	19
$(NH_4)_6P_2W_{18}O_{62}$	10	11
Semiconductor Systems		
TiO_2 (Degussa)	1	0
TiO_2 (Degussa)	2	0
TiO_2 (Degussa)[d]	1	0
TiO_2 (Degussa)[e]	1	0
TiO_2	1	0
TiO_2	2	0
TiO_2 (Degussa)/Pt[f]	1	0
TiO_2 (Aldrich)/Pt[g]	1	0
SnO_2	1	0
WO_3	1	0
CdS	1	0

[a] Irradiation time in all cases 16 h; source 550-W medium-pressure Hg-vapor lamp (see Experimental Section); reactions run in 5 mL of CH_3CN in 30-mL Schlenk flasks at 20 °C. [b] mol of THT/mol of photocatalyst (either polyoxometalate or semiconductor). [c] (1 − $[R_2S]_{end}/[R_2S]_0$) × 100, where $[R_2S]_{end}$ = quantity of thioether at end of irradiation; 0% means products below the detectable limit (yield <2%). [d] 10 μL of H_2O added to reaction mixture. [e] 40 μL of trifluoroacetic acid added to reaction mixture. [f] Degussa anatase TiO_2 with 10% Pt(0) (see Experimental Section). [g] Aldrich anatase TiO_2 with 10% Pt.

Anaerobic Photochemistry. Table I summarizes the relative efficiencies of these polyoxometalates and semiconductors with respect to photooxidizing a representative thioether, tetrahydrothiophene (THT), under anaerobic conditions. All the reactions employ the same solvent, acetonitrile, one minimally sensitive to oxidation by irradiated polyoxometalates or semiconductors, and the same temperature (20 °C throughout). The principal products in these anaerobic processes, with the exception of the reaction initiated by $Q_3PMo_{12}O_{40}$ are the α,α' dimeric coupling product and other species derived from the α-carbon radical of the thioether (eq 7). The product formed from the Keggin dodecamolybdophosphate reaction with dimethyl sulfide is (methylthio)methanol, CH_3SCH_2OH (eq 8). This product results from a two-electron oxidation and deprotonation of the substrate to generate the resonance-stabilized carbocation which, in turn, is trapped by rapid nucleophilic attack by water to generate the alcohol. Alcohol formation is seen in reactions of $Q_3PMo_{12}O_{40}$ with cyclooctane.[21] Oxygen atom abstraction from the polyoxomolybdate is also a

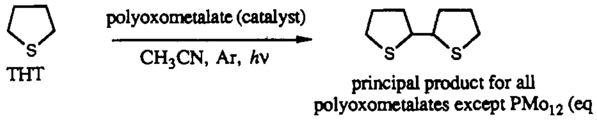

(7)

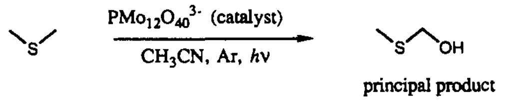

(8)

---

[17] (a) Calvert, J. G.; Pitts, J. N. *Photochemistry*; Wiley: New York, 1966. (b) Parker, C. A. *Proc. R. Soc. London* **1953**, *A220*, 104. Hatchard, C. G.; Parker, C. A. *Proc. R. Soc. London* **1956**, *A235*, 518.

[18] Baxendale, J. H.; Bridge, N. K. *J. Phys. Chem.* **1955**, *59*, 783.

[19] Personal communications from Drs. M. Grätzel and N. Serpone.

[20] Both $W_{10}O_{32}^{4-}$ and cubic WO_3 have a large number of corner-shared contacts between the WO_6 octahedra that comprise their structures.

[21] Hill, C. L.; Renneke, R. F.; Faraj, M. K.; Brown, R. B. In *The Role of Oxygen in Chemistry and Biochemistry*; Ando, W., Moro-oka, Y., Eds.; Elsevier: Amsterdam, 1988; pp 185–191.

Table II. Quantum Yields for Production of the Reduced Polyoxometalates and Oxidized Organic Product, 2,5-Dithiahexane, in the Homogeneous Photooxidation of Dimethyl Sulfide by Polyoxometalates[a]

polyoxometalate[b]	$\phi(P_{red})$[c]	ϕ(org)[d]
$Q_4W_{10}O_{32}$	0.022	0.017
$Q_3PMo_{12}O_{40}$	~0.005	
$Q_3PW_{12}O_{40}$	<0.002	

[a] Reaction conditions given in Experimental Section. [b] Q = tetra-*n*-butylammonium cation. [c] Defined as number of electron equivalents in reduced polyoxometalate divided by einsteins of photons absorbed by the oxidized catalyst (P_{ox}). [d] Defined as electron equivalents represented in the oxidized organic product formed, 2,5-dithiahexane, divided by einsteins of photons absorbed by P_{ox}.

possibility, but not likely. Neither sulfoxides nor sulfones, the usual products of thioether oxidation by oxometal species,[22] are produced under these anaerobic reaction conditions.[23] The latter products are produced, however, under aerobic conditions (vide infra).

Several things are clear from the reactions in Table I. First, all the semiconductor systems including Degussa anatase TiO_2 with or without Pt(0) are ineffective for thioether photooxidations under anaerobic conditions. This affirms observations made by many authors investigating the photochemical transformations of organic substrates by semiconducting metal oxides, namely, that in a great majority of the cases no detectable photochemistry is seen in the absence of O_2. In contrast to the semiconductor systems, all the polyoxometalates except the neutral quaternary ammonium salt form of dodecatungstophosphate, $PW_{12}O_{40}^{3-}$, do effect photochemical degradation of the substrate. The most reactive polyoxometalate examined in this study, $W_{10}O_{32}^{4-}$, derives its enhanced reactivity relative to the other polyoxometalates examined here from two effects. First, it exhibits higher quantum yields for photooxidation of the thioether substrate (see Table II) than the other polyoxotungstates and polyoxomolybdates in Table I, and second, it absorbs more light in the near-UV region of the absorption spectrum than the other complexes. The molar extinction coefficient for $W_{10}O_{32}^{4-}$ at 320 nm is 14000 M^{-1} cm^{-1};[11] those for $PW_{12}O_{40}^{3-}$ and $PMo_{12}O_{40}^{3-}$ at this wavelength are approximately 1400 and 22000 M^{-1} cm^{-1}, respectively.[24]

The quantum yields at 320 nm for the formation of the reduced polyoxometalate species with dimethyl sulfide were calculated by using ferrioxalate actinometry (see Table II). The quantum yield, Φ, is defined as the number of electron equivalents in the reduced polyoxoanion species divided by the einsteins of photons absorbed. The rates of reduced polyoxoanion formation for $Q_3PMo_{12}O_{40}$ and $Q_3PW_{12}O_{40}$ when irradiated with the 320-nm interference filter were too slow to monitor accurately. Values for these two photocatalysts were estimated by comparison with the $W_{10}O_{32}^{4-}$ reaction with full irradiance from the Xe arc lamp. This method assumes that the quantum yields for the different polyoxometalates are fairly constant over the whole LMCT region of their respective absorption envelopes. Quantum yields calculated for the formation of $W_{10}O_{32}^{6-}$ with cyclooctane as the substrate[4a,4f,11b] and for the formation of $PW_{12}O_{40}^{4-}$ with alcohols as the substrates[25] vary only slightly at different wavelengths in the LMCT region. The quantum yields for photoredox chemistry associated with the lower energy absorption bands of the reduced polyoxometalates are orders of magnitude smaller than quantum yields for photoredox chemistry associated with the LMCT chromophore of the oxidized polyoxometalates themselves and thus do not interfere with determination of the quantum yields of the latter.[25]

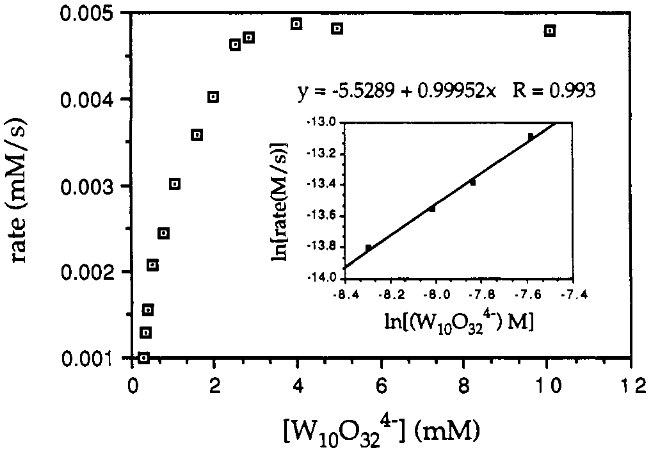

Figure 1. Dependence of the initial rate of THT photooxidation by $W_{10}O_{32}^{4-}$ on the concentration of $W_{10}O_{32}^{4-}$. The rate was determined by the initial-rate method as a function of $[W_{10}O_{32}^{4-}]$. Inset: ln–ln plot in the low-concentration and optically dilute regime. The equation just above figure is a least-squares equation approximating the data. [THT] = 0.1 M; T = 25 ± 2 °C; 3.0 mL of solution in a 2.0-cm cylindrical quartz Schlenk cuvette was irradiated under an inert atmosphere (see Experimental Section).

The quantum yield for formation of the principal organic product in the $W_{10}O_{32}^{4-}$/dimethyl sulfide system, 2,5-dithiahexane, was also calculated. The quantum yield in this case is defined as the equivalents of electrons represented in the oxidized organic product divided by the einsteins of photons absorbed by $W_{10}O_{32}^{4-}$. The value obtained in these calculations is less than the Φ calculated for formation of $W_{10}O_{32}^{6-}$. The higher quantum yields for the latter most probably derive from partial production of $W_{10}O_{32}^{6-}$ via oxidation of the organic quaternary ammonium countercations, used to solubilize the catalyst in the nonaqueous medium, by $W_{10}O_{32}^{4-*}$.

The lack of efficacy of the metal oxide semiconductors in these anaerobic photochemical thioether degradation reactions stems not only from the low effective concentration of the semiconductors in these heterogeneous reactions but also from the low thermal kinetic stability of the charge-separated excited forms of the semiconductors and the lack of efficient discharge of conduction band electrons. Note that the presence of neither an oxidatively resistant fairly strong acid, trifluoroacetic acid, nor the finely divided hydrogen evolution catalyst, Pt(0), facilitates the photochemical reactions with the semiconductors under anaerobic conditions (Table I). Unlike the semiconductors, the polyoxometalates form isolable multielectron-reduced forms; in addition, the reoxidation of these reduced forms by hydrogen evolution as in eq 3, or by aerobic reoxidation as in eq 5, can be controlled and used to initiate subsequent selective reactions.

The oxidative photochemical degradation of THT by the active polyoxotungstates under anaerobic conditions is sufficiently simple that rate measurements on such systems are satisfactorily reproducible and fairly informative. The kinetics of the most active system in this study, THT photooxidation by $W_{10}O_{32}^{4-}$ in acetonitrile solution, were examined. The techniques and limitations are described above (Experimental Section). In the optically dilute regime, this reaction proved to be first order in $W_{10}O_{32}^{4-}$, and in the optically dense regine, it proved to be approximately first order in light intensity[26] and variable order in THT substrate (Figures 1–3, respectively). The ln–ln plot of the THT dependence at low concentrations gives an order that is 0.6 in THT. At [THT] < 0.01 M, the order of the reactions in THT tends toward unity,

---

(22) Block, E. In *Chemistry of Ethers, Crown Ethers, Hydroxyl Groups and their Sulfur Analogues*; Patai, S., Ed.; Wiley: New York, 1980; Part 1, Chapter 13.

(23) Atom transfer, not electron transfer, is the principal mode of attack of polyoxotungstate excited states on ethers and thioethers: Chambers, R. C.; Hill, C. L. *J. Am. Chem. Soc.* **1990**, *112*, 8427. Chambers, R. C.; Prosser-McCartha, C. M.; Hill, C. L. Unpublished work.

(24) The molar extinction coefficients of $PW_{12}O_{40}^{3-}$ and $PMo_{12}O_{40}^{3-}$ at this wavelength were measured for this study.

(25) Dimotikali, D.; Papconstantinou, E. *Inorg. Chim. Acta* **1984**, *87*, 177.

(26) In this case ln (rate) versus ln (% full light intensity) has been plotted. While this plot is not as quantitative as a plot of ln (rate) versus ln (% irradiance), where irradiance is the radiant power incident on a surface divided by the area of the surface (W/m^2 or equivalent units), the former plot is satisfactory to rule out a dominant biphotonic photochemical pathway.

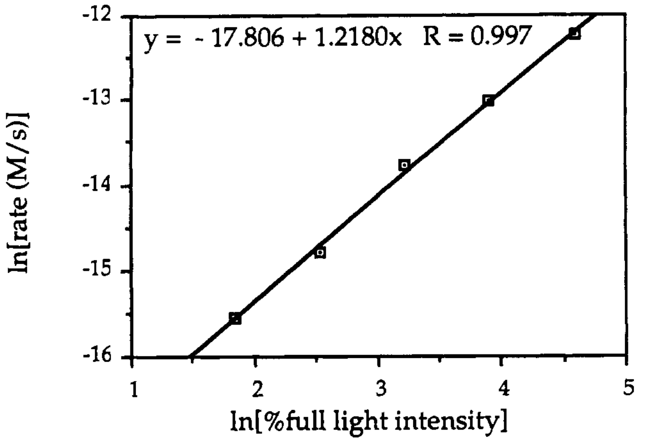

Figure 2. Dependence of the initial rate of THT photooxidation by $W_{10}O_{32}^{4-}$ on light intensity (% full intensity of light source). Values were obtained at 630 nm under optically dense conditions ($[W_{10}O_{32}^{4-}]$ = 5 mM, [THT] = 0.1 M; T = 25 ± 2 °C) using UV neutral-density transmittance filters (50%, 25.1%, 12.6%). 3.0 mL of solution in a 2.0-cm cylindrical quartz Schlenk cuvette was irradiated under an inert atmosphere (see Experimental Section).

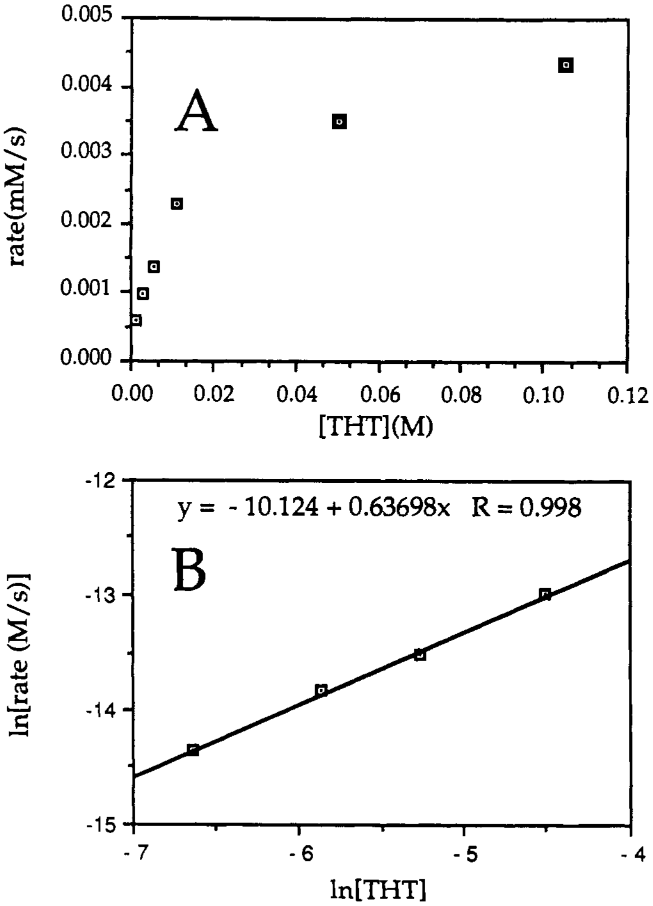

Figure 3. (A) Dependence of the initial rate of THT photooxidation by $W_{10}O_{32}^{4-}$ on [THT] under optically dense conditions ($[W_{10}O_{32}^{4-}]$ = 5 mM). (B) ln-ln plot at lower THT concentrations. 3.0 mL of solution in a 2.0-cm cylindrical quartz Schlenk cuvette was irradiated under an inert atmosphere (see Experimental Section).

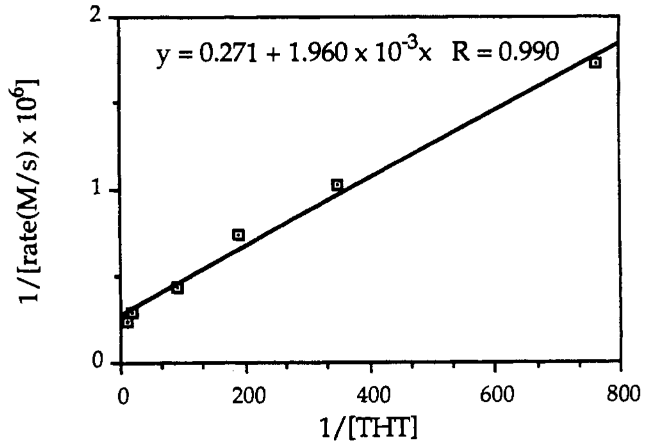

Figure 4. Plot of 1/rate (M/s) versus 1/[THT]. Experimental conditions were same as for Figure 3.

while at [THT] > 0.3 M, the order in substrate tends toward zero. Determination of an accurate and precise value for the order of the reaction in THT becomes problematic at low concentrations of substrate; the background oxidation of acetonitrile solvent accounts for 50% of the reduced complex generated at [THT] ≤ 1 mM.

A minimal mechanism and rate law consistent with the rate data (including saturation kinetics in THT substrate) and the products (principally the dimer, $(THT[-H])_2$, at early reaction times) are given in eqs 9–14 and eq 15, respectively. The symbols

$$W_{10}O_{32}^{4-} + h\nu \xrightarrow{\phi I} W_{10}O_{32}^{4-}* \qquad (9)$$

$$W_{10}O_{32}^{4-}* \xrightarrow{k_{ic}} W_{10}O_{32}^{4-} \qquad (10)$$

$$W_{10}O_{32}^{4-}* + THT \xrightarrow[slow]{k} W_{10}O_{32}^{5-} + THT[-H]\cdot + H^+ \qquad (11)$$

$$2\,THT[-H]\cdot \longrightarrow (THT[-H])_2 \qquad (12)$$

$$2\,W_{10}O_{32}^{5-} \longrightarrow W_{10}O_{32}^{4-} + W_{10}O_{32}^{6-} \qquad (13)$$

$$(THT[-H])_2 \longrightarrow \text{further oxidation} \qquad (14)$$

$$\text{Rate} = +d/dt[W_{10}O_{32}^{6-}] = k\phi I[THT] / k[THT] + k_{ic} \qquad (15)$$

Φ and I (eqs 9 and 15) and k_{ic} (eqs 10 and 15) stand for the quantum efficiency for production of the photoredox-active excited state of $W_{10}O_{32}^{4-}$, the rate of light absorption by this complex, and the rate constant for deactivation of the excited state by internal conversion, respectively. Although there are other excited-state decay processes, internal conversion is by far the dominant process. The rate law described in eq 15 predicts that the plot of 1/rate versus 1/[THT] will be linear. This was borne out by the experimental data (Figure 4). Data from Figures 3 and 4 lead to a value of $k_{ic} \sim 1.1 \times 10^{11}$ s^{-1}, in good agreement with the only measured lifetime of the excited state of $W_{10}O_{32}^{4-}$ yet available: 21 ps in acetonitrile or water solution at 25 °C (355-nm excitation).[27]

Aerobic Photochemistry. The addition of dioxygen to any of the catalytic anaerobic reactions described above results in more rapid and more complete photochemical oxidative degradation of THT and other thioethers. Exemplary reactions with both types of systems are summarized in Table III. In the presence of O_2 (for conditions see the Experimental Section and Table III), all the semiconductor systems except WO_3 and CdS lead to extensive photochemical decomposition of THT, with the Degussa TiO_2 anatase being the most effective. Neither sulfoxides nor sulfones are seen as products with the latter semiconductor (yields ≪1%). This is not surprising, given the known ability of this particular semiconductor to effect complete mineralization of some organic

---

[27] The lifetime in solution of the weakly emissive excited state of $W_{10}O_{32}^{4-}$, generated upon excitation at 355 nm, has been measured in acetonitrile and water at 25 °C in two different laboratories to be approximately 2.1 × 10^{-11} s (Kozik, M.; Winkler, J.; Hilinski, E. F.; Tate, K.; Duncan, D.; Hill, C. L. Unpublished work). A caveat concerning the utility of this value: the only solvents that are compatible with all the photochemistry here, water and acetonitrile, quench the excited state. Further work is in progress.

Table III. Photochemical Decomposition of Tetrahydrothiophene (THT) under Aerobic Conditions Catalyzed by Various Catalysts[a]

catalyst	mole ratio[b]	% decompn[c]
Polyoxometalate Systems		
$Q_4W_{10}O_{32}$	20	~100
$Q_3PMo_{12}O_{40}$	10	<1
$Q_3PW_{12}O_{40}$	10	0
$Q_4SiMo_{12}O_{40}$	10	8
$Q_5PV_2Mo_{10}O_{40}$	10	7
$H_5PV_2Mo_{10}O_{40}$	10	46
$Q_5Cu^{II}W_{11}PO_{39}$	10	12
$(NH_4)_6P_2W_{18}O_{62}$	10	12
Semiconductor Systems		
TiO_2 (Degussa)	1	80
TiO_2 (Degussa)	2	63
TiO_2	1	35
TiO_2	2	26
SnO_2	1	10
WO_3	1	0
CdS	1	0

[a] Irradiation time in all cases 4 h; source 1000-W Xe arc lamp with 340-nm cutoff and circulating infrared water filters (see Experimental Section); reactions were run in 5 mL of CH_3CN in 30-mL Schlenk flasks. [b] mol of THT/mol of photocatalyst (either polyoxometalate or semiconductor). [c] $(1 - [R_2S]_{end}/[R_2S]_0) \times 100$, where $[R_2S]_{end}$ = quantity of thioether after irradiation; 0% means products below the detectable limit (yield <2%).

compounds under similar conditions.[1d,2d] It is not surprising that the reactivities of the different semiconductors do not correlate with their band gaps. The band gaps, approximated by values measured when the semiconductors are in contact with aqueous electrolyte at pH 1,[28] and the reactivities are as follows: TiO_2, 3.2 eV, most reactive; SnO_2, 3.8 eV, somewhat reactive; WO_3, 3.2 eV; unreactive; CdS, 2.5 eV, unreactive. Although the amount of light absorbed by the different semiconductors is not constant, the biggest factor in the different levels of effectiveness of the semiconductors in the aerobic reactions, given the complete lack of reactivity of all of them under anaerobic conditions, is not the inherent reactivities of their excited states to attack the substrate. Rather, it is the relative abilities of the various semiconductors to modulate the reactions of O_2 and O_2-derived oxidants including the chain-carrying peroxy radicals that are doubtless intermediates in the more active processes (i.e. those with TiO_2).

The reactive polyoxometalates in the presence of O_2 produce low yields of sulfoxide and sulfone and several unidentifiable products. More significantly, it is clear that many of the initial organic products are unstable under the reaction conditions, rendering the quantification of the organic products a marginally useful exercise. The nonacidic complexes $PMo_{12}O_{40}^{3-}$ and $PW_{12}O_{40}^{3-}$ lead to virtually no detectable removal of the thioether substrate under the brief conditions of irradiation used in the aerobic reactions (Table III). The reported lower level of reactivity of $PMo_{12}O_{40}^{3-}$ in the aerobic versus the anaerobic reactions derives from two experimental points—all the aerobic reactions were irradiated for shorter periods of time than their anaerobic counterparts (4 versus 16 h) and with lower energy light ($\lambda > 340$ nm versus $\lambda > 280$ nm = Pyrex cutoff). The isopolyoxotungstate, $W_{10}O_{32}^{4-}$, is the most effective system of all those evaluated under aerobic conditions, as it was under anaerobic conditions. The low toxicity of this and many other polyoxotungstates[29] and the accessibility of these materials in quantity from inexpensive starting materials suggest possible uses of these compounds in photocatalytic decontamination technology.

Acknowledgment. We thank the U.S. Army Research Office (Grant No. DAAL03-91-G-0021) for support of this work. We thank Yuqi Hou in our group for the sample of cubic WO_3.

---

(28) Reference 1d, pp 100–101.

(29) (a) Chermann, J. C.; Jasmin, C.; Mathe, G.; Raynaud, M. French Patent 58693/71. (b) Hill, C. L.; Hartnup, M.; Faraj, M.; Weeks, M.; Prosser-McCartha, C. M.; Brown, R. B.; Schinazi, R. F.; Sommadossi, J.-P. In *Advances in Chemotherapy of AIDS, Pharmacology and Therapeutics*; Diasio, R., Sommadossi, J.-P., Eds.; Pergamon: New York, 1990; pp 33–41. (c) Hill, C.; Weeks, M.; Schinazi, R. F.; *J. Med. Chem.* **1990**, *33*, 2767.

Contribution from the Chemistry Department, University of Kuwait, Box 5969, 13060 Safat, Kuwait, and Department of Chemistry, University of Helsinki, Et. Hesperiankatu 4, 00100 Helsinki, Finland

MS Xα Studies on the Colors of $BiPh_5$, $PbCl_6^{2-}$, and WS_4^{2-}: Are Relativistic Effects on the LUMO Important?

B. D. El-Issa,[†] P. Pyykkö,[*,‡] and H. M. Zanati[†]

Received June 21, 1990

Quasirelativistic multiple-scattering Xα (MS Xα) and pseudopotential Hartree–Fock calculations are performed on MX_5 (M = Bi, Sb; X=H, CCH) model systems in D_{3h} or C_{4v} site symmetries to elucidate the origin of the violet color of pentaphenylbismuth. The occurrence of this color only for Bi and for C_{4v} symmetry is related to the relativistic stabilization of the a_1 LUMO as concluded earlier from REX calculations. The nonrelativistic transitions are symmetry-forbidden. The relativistic perpendicular C_{4v} transition is allowed, in agreement with experiment. The study is extended further to include MS calculations on octahedral and tetrahedral site symmetries. The yellow color of $PbCl_6^{2-}$ is also attributed to the relativistic stabilization of the a_{1g} LUMO. The color difference between MoS_4^{2-} and WS_4^{2-} is mainly due to the shell-structure effects and not relativity.

1. Introduction

Pentaphenylbismuth was synthesized by Wittig and Clauss[1] in 1952. This compound shows an intense violet color, an unusual phenomenon for a main-group organometallic compound in its highest oxidation state. Seppelt et al.[2,3] have recently considered the origin of this color. They found that it never occurs in the lighter MR_5 congeners of Bi, such as Sb, and never occurs when the site symmetry of Bi is D_{3h}. Thus a necessary condition for this absorption is that the metal be bismuth and the site symmetry C_{4v}. A simple comparison of relativistic and nonrelativistic extended Hückel calculations on MH_5 model systems suggested that

---

[*] To whom correspondence should be addressed.

[†] University of Kuwait.

[‡] University of Helsinki.

(1) Wittig, G.; Clauss, K. *Liebigs Ann. Chem.* **1952**, *578*, 136.

(2) Schmuck, A.; Buschmann, J.; Fuchs, J.; Seppelt, K. *Angew. Chem.* **1987**, *99*, 1206; *Angew. Chem., Int. Ed. Engl.* **1987**, *26*, 1180.

(3) Schmuck, A.; Pyykkö, P.; Seppelt, K. *Angew. Chem.* **1990**, *102*, 211; *Angew. Chem., Int. Ed. Engl.* **1990**, *29*, 213.

0020-1669/91/1330-2781$02.50/0